available at www.sciencedirect.com

ScienceDirect

journal homepage: www.elsevier.com/locate/ijrefrig

Attempt of integration of a small commercial ammonia-water absorption refrigerator with a solar concentrator: Experience and results

A. Busso [a,*], J. Franco [b], N. Sogari [a], M. Cáceres [a]

[a] GER, Grupo en Energías Renovables, FaCENA-UNNE, Av. Libertad 5470, 3400 Corrientes, Argentina
[b] INENCO-CONICET, UNSa, Salta, Argentina

ARTICLE INFO

Article history:
Received 20 April 2010
Received in revised form
14 June 2011
Accepted 18 July 2011
Available online 2 August 2011

Keywords:
Ammonia
Absorption system
Solar refrigeration
Solar concentration
Thermodynamic property

ABSTRACT

The integration of a small commercial ammonia-water absorption refrigerator with a solar concentrator as heat source was analyzed theoretically and experimentally. Operation parameters of the fridge were determined by parametric fitting experimental data using a thermodynamic model of the cycle leading to a working pressure of 25 bar, weak and strong solution concentrations of 15% and 30% respectively and a COP of ~0.18. As sold, the fridge can operate with a reduction in the electric power supply of up to 40%. Results showed that the Parabolic Concentrator (PC) used can deliver temperatures above 200 °C for almost 6 h with an average useful power delivery and efficiency of 530 W and 26% respectively. During laboratory test runs it was possible to hold the refrigeration cycle running in a very unstable regime despite the inappropriate heat distribution in the generator unit due to the lower temperature heat source used (220 °C). However, outdoor testing with the sun as energy source proved unsuccessful due to the higher heat losses that occur at the pipes connecting the PC with the fridge.

Tentative d'intégration d'un réfrigérateur commercial à absorption à ammoniac / eau de petite taille et d'un capteur solaire : expérience acquise et résultats

Mots clés : Ammoniac ; Système à absorption ; Froid solaire ; Concentration du rayonnement solaire ; Propriété thermodynamique

* *Corresponding author*. Tel.: +54 3783 473931x116; fax: +54 3783 473930.
E-mail address: ajbusso@gmail.com (A. Busso).
0140-7007/$ – see front matter © 2011 Elsevier Ltd and IIR. All rights reserved.
doi:10.1016/j.ijrefrig.2011.07.004

Nomenclature

a_i	Coefficients
A	Surface area (m^2)
h	Specific enthalpy (kJ kg^{-1})
k	Thermal conductivity of wall material (W-m^{-1}-$°C^{-1}$)
M	Molar weight (kg mol^{-1})
p	Pressure (MPa)
q	Heat transfer rate through a wall (W)
Q	Energy rate (W)
T	Temperature (°C)
ΔT	Temperature difference (°C
ΔX	Wall thickness (m)
x	Ammonia mol fraction in the liquid phase
y	Ammonia mol fraction in the gas phase
w	Ammonia mass fraction in the gas phase

Greek letters

ε	Ratio between temperature-to-power variations of a given cycle component
η	efficiency

Abbreviations

CNEA	Comisión Nacional de Energía Atómica
COP	Coefficient Of Performance
DAR	Diffusion–Absorption Refrigerators
GES	Grupo de Energía Solar
INENCO	Instituto Nacional de Energía No Convencional
LPC	Liner Parabolic Concentrator
LPG	Liquefied Petroleum Gas
PC	Parabolic Concentrator
PET	Polyethylene Terephtalate
UNNE	Universidad Nacional del Nordeste
UNSa	Universidad Nacional de Salta
UNSE	Universidad Nacional de Santiago del Estero
UNF	Universidad Nacional de Formosa

Subscripts

amb	ambient
Am	ammonia
abs	absorber
av	average
bp	bubble pump
cab	cabinet
cond	condenser
evap	evaporator
fr	freezer
fg	flue gas
g	gas phase
gain	gain
gen	generator
hx	heat exchanger
i	term i of polynomial
in	inlet
l	liquid phase
ls	loss
out	outlet
total	total
useful	useful
W	water
ws	water separator
0	reference value

1. Introduction

The application of solar energy for the production of cold is a field with high potential in the years to come. By reason that solar refrigeration technologies have the advantage of removing the majority of harmful effects of traditional vapor compression refrigeration machines and that the peaks of requirements in cold coincide most of the time with the availability of the solar radiation, the development of solar refrigeration technologies became the worldwide focal point of concern again (Fan et al., 2007).

Within this context, the water-ammonia (NH_3–H_2O) absorption cycle is a technology based on the wide-ranging experience gathered in the early years of the refrigeration industry, particularly for ice production and food preservation. This technology dates back to the 1920s when a device called the "Icy-Ball Refrigerator" (Keith, 1927) was patented and marketed in the U.S. and Canada. The device was unusual in design in that it did not require the use of electricity for cooling. It ran for a day on about a cup of kerosene allowing rural users lacking electricity to utilize the benefits of refrigeration. Through the following years technological developments led to the integration of components and into a refrigerator which found widespread use in rural areas with its burner normally operated on gas, kerosene or even biomass.

Some distinguishing features of the ammonia-water cycle are: a) it is made up of relatively simple components; b) ease of working with a variety of energy sources (gas, kerosene, solar, biomass); c) low generator working temperature, approximately 120 °C; These features make the absorption cycle a good candidate to work in conjunction with solar energy.

Furthermore, the use of solar energy in refrigeration for preservation of perishable goods has the following advantages: a) the use of a free and clean resource significantly reduces operating costs; b) there is a good correlation between availability of the solar resource and cooling demand minimizing or eliminating the need for energy storage; c) pollution free energy source; d) it presents a good alternative to improve the quality of life of residents in remote rural areas; e) solar energy can be supplied to the cooling system by a solar collector, concentrating collectors being the most appropriate since they can reach temperatures over 300 °C.

In Argentina both technologies, ammonia-water absorption cooling and solar concentration, are available and proven with many years of experience. Absorption refrigerators powered by a variety of energy sources (LPG burner, kerosene or biomass) have been commercially available and in use in rural areas for more than 50 years. Furthermore, the solar concentration have been extensively studied at INENCO – Instituto Nacional de Energía no Convencional (Hoyos et al.,

1999; Echazú et al., 2000; Saravia and Suárez, 2000; Cadena and Saravia, 2001; Saravia, 2002; Cadena et al., 2002; Saravia et al., 2004a,b). They have developed a Parabolic Concentrator (PC) for cooking purposes which has been tested with success at operating temperatures above 300 °C (Saravia et al., 2004a,b).

With this background in mind it seemed interesting attempting to combine both technologies and analyze, theoretically and experimentally, the feasibility of running a commercial refrigerator with the sun as a heat source.

In the following paragraphs results and main conclusions of the work carried out with the objective of integrating a small commercial domestic ammonia-water absorption refrigerator with a solar concentrator as a thermal power source are presented. Reengineering the technologies to be used was at no time considered within the objectives of the authors although the results obtained may indicate the need for this. As a byproduct of this research an electric energy economizer was implemented and successfully tested (Cáceres et al., 2009).

This study is part of a collaborative program carried out by four universities [UNNE, UNSa, UNSE, UNF] and aimed at applying renewable energy technologies to improve the life of inhabitants of the Great Chaco Plain in Northern Argentina.

2. Technologies involved

2.1. *Absorption refrigeration*

An absorption refrigerator is a refrigerator that uses a heat source (e.g., electric heater, solar, kerosene-fueled flame) to provide the energy needed to drive the cooling system. Absorption refrigerators represent a popular alternative to regular compressor refrigerators where electricity is unreliable, costly, or unavailable, where noise from the compressor is problematic (hotel mini-bars), or where surplus heat is available (e.g., from turbine exhausts or industrial processes). For example, absorption refrigerators powered by heat from the combustion of liquefied petroleum gas (LPG) are often used for food storage in recreational vehicles and rural areas with no grid coverage.

The phenomenon of absorption is based on the ability of certain substances in liquid phase that, under specific conditions of pressure and temperature, can uptake large quantities of gases of other substances, thus forming a saturated solution usually called “strong solution”. This process of absorption generates some heat. The reverse procedure, desorption, requires a heat source to separate the gas from the liquid leaving behind a weaker solution as a result. These two effects combined are capable of replacing the compressor in the conventional vapor compression refrigeration thus leading to the absorption refrigeration cycle. Furthermore, the ammonia-water cycle has features that make it a good candidate to work in conjunction with thermal solar energy devices as a heat source.

Absorption cooling was invented by the French scientist Ferdinand Carré in 1858. The conventional absorption cycle in its original form is dependent upon mechanical energy, as it uses a pump to maintain the pressure difference between the evaporator side and the condenser side. In order to make a fully autonomous machine the Swedish engineers Carl Munters and A. von Platen, in the 1920s (Herold et al., 1996), conceived the well-known Servel-Electrolux diffusion–absorption cycle, with key features such as running continuously without moving parts and being driven by heat only. The cycle is based on the principle of pressure equilibration between the high and low pressure sides of the unit through an inert auxiliary gas such as helium or hydrogen. A further peculiarity of this type of absorption cooling machine, is the use of a thermally driven gas bubble pump for the circulation of the solution cycle instead of a mechanical solution pump, so that inside the cooling machine no mechanically moving parts are necessary.

These small, simply constructed cooling machines, either driven by electrical heating cartridges or direct flame with a simple mechanical construction, do not need conventional high-performance pumps or expansion valves, but show a very low coefficient of performance (COP) and therefore high energy consumption.

The gas, kerosene or electrically driven diffusion–absorption refrigerators (DAR) were theoretically and experimentally investigated in numerous research projects concerning refrigeration applications (Almén; Chen et al., 1996; Jakob et al., 2008; Kouremenos et al., 1994; Kim et al., 1995; Smirnov et al., 1996; Srikhirin and Aphornratana, 2002; Vicatos, 2000).

Fig. 1 sows a general scheme of the Platen-Mounters process with the different components of the cycle. A single-pressure unit is charged with water, ammonia and usually hydrogen as inert gas. At standard atmospheric conditions, ammonia is a gas with a boiling point of −33 °C, but a single-pressure absorption refrigerator is pressurized to the point where ammonia is a liquid. The cycle is closed, with all hydrogen, water and ammonia collected and endlessly reused. There are no pressure differences in the unit except those caused by liquid columns. The total pressure, sum of partial pressures of ammonia and hydrogen, is constant at all points of the system and therefore there is no need for any expansion valves. The condenser is situated above the evaporator, so the ammonia condensate flows by gravity from one to the other. The difference in height, h_1, is not due to any flow resistance but to the fact that the liquid in the left leg of the tube is colder and thus denser.

The cooling cycle starts with liquefied ammonia entering the evaporator. At the cold end of the evaporator enters weak gas, i.e. hydrogen with a low concentration of ammonia vapor (i.e. low partial pressure), together with liquid ammonia from the condenser at a rate of a few droplets per second. The partial pressure of the hydrogen is used to regulate the total pressure, which in turn regulates the vapor pressure and thus the boiling point of the ammonia. The liquid ammonia wets the surface of the tube and assumes the temperature of the tube wall. The temperature determines the vapor pressure of ammonia close to the liquid surface. If the partial pressure of ammonia in the gas away from the wall is lower, then the vapor tends to migrate from higher to lower concentration – a diffusion process. As there is a steady supply of weak gas, the difference of vapor pressure (on the wall - in the gas) is maintained, which causes a steady evaporation of the liquid. The evaporating molecules are the ones with most energy/velocity and the ones left behind with (on an average) less energy are colder. So the evaporation causes a drop of

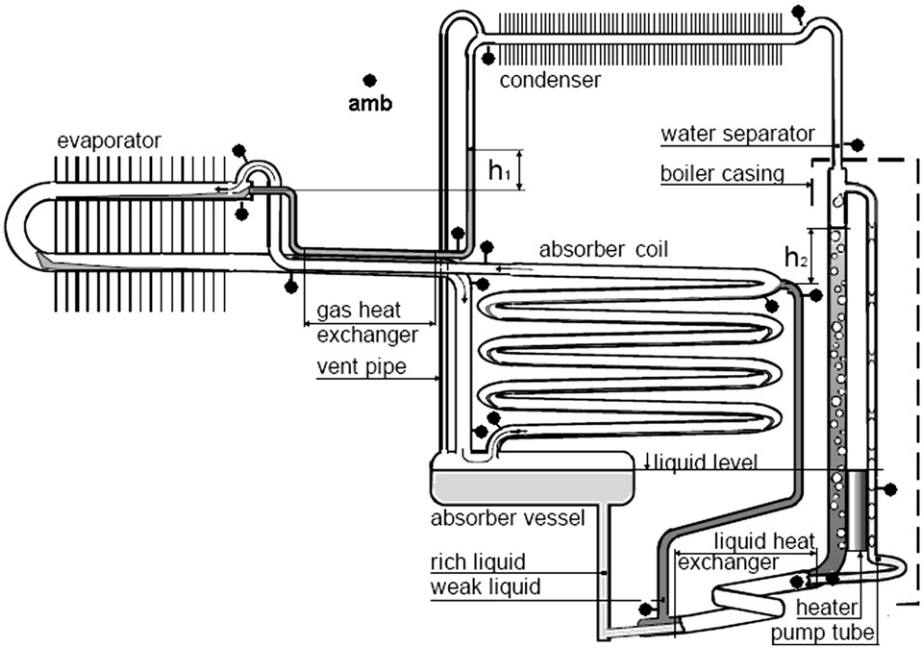

Fig. 1 – Scheme of the Platen-Munters absorption refrigeration unit (source Almén, Chp.1). The black dots indicate the locations of the temperature sensors during experiments.

temperature of the liquid and the tube wall. This is the refrigerating effect of the evaporation. By this, the density of the gas mixture increases (ammonia vapor is 8.5 times heavier than hydrogen) and tends to flow downwards to the absorber coil, situated further down.

So the basic process in the evaporator is diffusion of ammonia vapor driven by a concentration gradient, away from the liquid surface into the gas stream, and as a consequence of this, we have the refrigeration which is basically the evaporated mass flow by the heat of evaporation of NH_3.

If no special measures are taken, the liquid flows in a small stream at the bottom of the evaporator tube and over it forms a layer of rich gas. As NH_3 vapor is 8.5 times heavier than H_2, the rich gas is heavier than the average mixture in the tube and a stable stratification of the gas develops at the bottom, reducing the heat transfer and hence evaporation.

The next three steps exist to separate the gaseous ammonia and the hydrogen. First, in the absorber, the mixture of gasses enters the bottom of an uphill series of tubes, into which a weak solution whose mass fraction is ~15% (Isaza, 2004; Kwan et al., 1995) is added at the top. The ammonia dissolves in the weak solution, producing a mixture of ammonia solution and hydrogen. In this process hydrogen gets lighter and tends to flow upwards to the evaporator. Hence, the hydrogen is collected at the top of the absorber and the resulting strong ammonia solution whose mass fraction is ~30% (Isaza, 2004; Kwan et al., 1995) collected at the bottom of the absorber. Here we have the gas loop between evaporator and absorber and a natural circulation of the gas due to the density differences.

The second step is to separate the ammonia and water. There is a heater tube in the distillation apparatus or boiler as it is normally called in the context of Platen-Munters units. The tube can be seen either as a receptacle for an electric heater or as part of a flue tube. It properly heats a pump tube (bubble pump) which has a small internal diameter (usually 3.5–5 mm) as well as the "distillation column". In the bubble pump, part of the ammonia is boiled out of the solution and the bubbles force the liquid to rise as indicated in Fig. 1. The liquid must be pumped up to a certain height of the distillation column, and here besides, it must be pumped high enough to allow it to flow back to the top of the absorber by gravity (the height h_2 is necessary due to density differences). For this Platen and Munters used a thermosyphon pump. In this distillation process some water remains with the ammonia in the form of vapor and bubbles. This is dried in the final separation step, called the water separator, by passing it through an uphill series of twisted pipes with minor obstacles to pop the bubbles, allowing the remaining water to condense and drain back to the generator.

Finally the pure ammonia gas enters the condenser. Air circulating over the fins of the condenser removes heat from the ammonia vapor cooling it down to room temperature and hence condenses to a liquid, allowing the cycle to restart.

The weak ammonia solution coming out of the boiler, has a temperature of, typically, 180 °C and the rich ammonia solution from the absorber vessel typically 50 °C, so the liquid heat exchanger in between, improves performance and efficiency. When the hydrogen passes through the absorber, it warms to, say, 50 °C. When it passes through the evaporator it cools off to, say −10 °C. This heating and cooling causes a loss of refrigeration, and the gas heat exchanger is vital for performance (without such exchanger, there would be no useful refrigeration left).

When the unit enters in operation for the first time, there is hydrogen in all parts. When the ammonia vapor starts to flow from the boiler, the hydrogen is expelled from boiler and condenser through the vent pipe to the evaporator-absorber

and the overall pressure increases somewhat. If the ambient temperature is low, the condenser has surplus capacity and some hydrogen will linger in the last part of it.

If the ambient temperature is high enough, the condenser will not have enough capacity to condense all vapor, so some uncondensed vapor will spill over to the absorber through the vent.

Heat is generated in the absorber by the process of absorption. This heat must be dissipated into the surrounding air. Heat must also be dissipated from the condenser in order to cool the ammonia vapor sufficiently for it to liquefy. Free air circulation is therefore necessary over the absorber and condenser.

The whole unit operates by the heat applied to the generator system and it is of paramount importance that this heat be kept within the necessary limits and is properly applied.

2.2. *Solar concentrator*

A solar concentrator similar to the one developed for cooking purposes at the INENCO - National Institute of Non-Conventional Energy in Norwest Argentina (Cadena et al., 2002), capable of reaching temperatures of up to 400 °C in its focus became an interesting alternative to power a small commercial absorption refrigerator. Fig. 2 shows a front view picture of this concentrator. The mirror surface is made with strips of high reflectivity polished aluminum sheet used in commercial lighting units. These strips are conveniently mounted and fixed onto a light weight skeleton constructed with structural rectangular steel pipe with the shape of the PC. The device has an aperture area of 2 m^2 and is manually rotated along two axis thus enabling sun tracking.

The results of field experiments performed by Saravia et al. (2004a) with fluid temperatures in the range between 100 °C and 300 °C showed that the concentrator can deliver energy with an efficiency of 50%–25% respectively, during an interval of 8–9 h of continuous operation. In this way, it may be expected that with a solar radiation of 1000 W m^{-2} an aperture area of 2 m^2 and operating temperatures in the tested range, the solar collector could deliver a power output between 1000 W and 500 W.

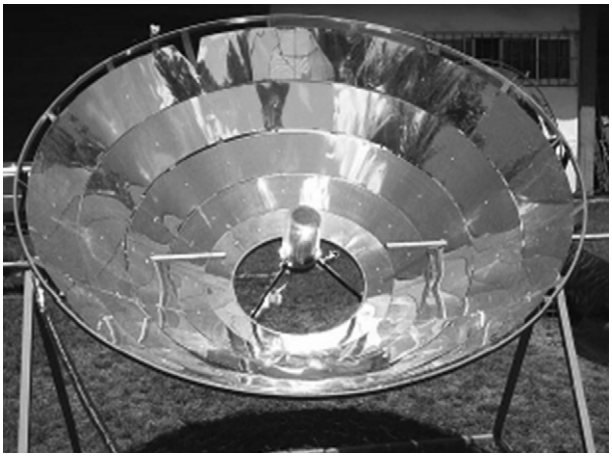

Fig. 2 – Front view of the solar concentrator and boiler setup.

3. Experimental setup

3.1. *Proposed integration scheme*

Gaia et al. (1999) proposed an integration scheme comprising two hydraulic circuits, indirectly coupled via heat exchanger immersed in a large heat storage tank. In contrast, to avoid unnecessary heat losses we propose only a small heat transfer fluid intermediary tank with the PC directly attaching to the fridge. Fig. 3 depicts the proposed integration scheme. During the components characterization stage of the research the PC and fridge were tested independently from each other. During laboratory testing of the fridge an electrical heater is installed inside the intermediary tank to emulate the PC as heat source. The temperature control of the heat transfer fluid in the boiler located at the focal point of the PC is accomplished by varying the revolution per minute (rpm) of the gear pump.

3.2. *Main components and power requirements estimation*

Both technologies, PC and absorption refrigeration, are not widespread in Argentina's market and much less is the technical information provided by the available few manufacturers. Therefore, the selection of these components have been done by comparing the power output of INENCO's tested PC with the power demand of a known commercial absorption refrigerator. Table 1 describes the technical specifications of the selected fridge and PC.

Based on this information, an estimation of the fridge's daily gas and electric demand leads to an ultimate power consumption of 203 W and 120 W respectively. We assume that the

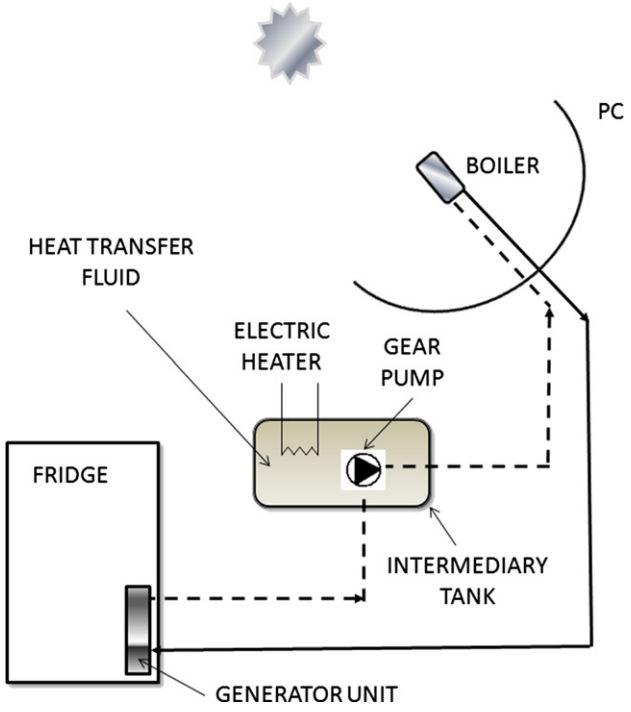

Fig. 3 – Proposed integration scheme for the combined system.

Table 1 – Technical specifications of the fridge and PC.

Component	Specifications		
Refrigerator	Model: TRIAL HG 60	Height: 1.050 m Width: 0.57 m	Consumption (according to manufacturer) Gas: 380 gr/24 h (Propane)
Cycle Ammonia-Water	Manufacturer: BERCOMAR Argentina	Depth: 0.67 m Capacity: 150 l	Power at 12 V: 120 W Operation temperature: ~120 °C
Solar PC	Manufacturer: INENCO – National Institute of Non-Conventional Energy. National University of Salta. Argentina	Diameter: 1.690 m Aperture area: ~2 m^2	Efficiency: (Saravia et al, 2004a,b) @ 100 °C = 50% @ 300 °C = 25%

incongruity may be due to the heat transfer losses when operating with gas leading thus to an optimistic burner efficiency of about 60%. It is to be noted that the temperature measured at inner side wall housing of either source is about 350 °C.

According to the results of Saravia et al. (2004a), a PC with an aperture area of 2 m^2 operating at a fluid temperature of 300 °C, delivers 500 W which implies a power availability more than enough to meet the fridge consumption as determined previously. Although 300 °C falls a bit below the operational temperature measured for the heat source supplied with the fridge, Saravia suggests that the PC can reach higher temperatures.

3.2.1. *PC and hydraulic system*

Fig. 2 shows a photograph of the proposed PC-boiler setup. The boiler unit comprises the collecting coil and a transparent cover. The coil is made out of a copper pipe of 0.019 m in diameter, bent in a coil shape with 10 turns in close contact with each other. The arrangement is smoke black coated to increase the absorbance of the sunlight that strikes the surface. A Pyrex® glass beaker with a length of 0.25 m and a diameter of 0.13 m is used as transparent cover so as to reduce heat losses. The boiler setup is rigidly mounted at the focal point of the PC. To allow the free movement of the PC around its axis of rotation the outputs of the coil are connected to the intermediary storage tank through flexible stainless steel pipe with a diameter of 0.019 m. The entire hydraulic circuit is thermally insulated with a layer of fiber glass wool 0.05 m thick. A gear pump immersed in the thermal oil inside the intermediary tank forces the fluid to flow through the hydraulic circuit. The pump is driven by a motor-gearbox assembly taken from a car electric window mechanism with a measured power demand of 21 W. Two different heat transfer fluids were used in the hydraulic system during tests, Cauquen I, produced by Repsol YPF and ESSOTHERM 500, produced by ESSO. Both thermal fluids have a boiling range above 300 °C according to the technical specifications provided by the manufacturers. The volume of oil contained in the circuit is approximately 7 L. An electric heater with a power of 1250 W was placed inside the intermediary tank to enable the operation of the fridge with hot oil during the laboratory testing stage.

3.2.2. *Refrigerator*

Table 1 presents the technical specifications provided by the manufacturer. Photographs of the front and rear side of the fridge used are shown in Fig. 4 where main cycle components are identified. The electric heater is a two point resistance with values of 1Ω or 173Ω depending on the input voltage source. The desired supply voltage is selected with a switch that enables the resistance of 1Ω for 12 V DC or the resistance of 173Ω for 220 V AC. The heater is housed inside an iron pipe which is welded to a smaller diameter pipe that conform the bubble pump (Fig. 5a). The flue gas pipe follows a similar arrangement consequently the heat developed by either source (gas/electric heater) is transferred to the bubble pump through the welded area thus making the heat transfer process rather inefficient. The sketch on Fig. 5b depicts the thermal link between components of the generator set. Another drawback of this fridge is the lack of regulation of the electric power injection. In the electric mode the heater operates all the time at full power, not being the case in the gas mode, in which a thermostatic valve regulates the intensity of the flame and thus the heat supplied to the generator.

In order to power the fridge with hot oil from the PC a heat exchanger had to be designed and implemented. Due to the geometric complexity of the generator unit the heat exchanger was developed using the steel pipe housing of the electric heating cartridge. The heating cartridge was removed and the pipe was sealed at both ends with a couple of specially designed connectors acting as inlet and outlet so as to allow free circulation of the heating fluid in the circuit. Fig. 5c shows a schematic description of this heat exchanger setup.

4. Measuring instrumentation

In order to ensure proper PC-fridge integration the optimal working parameters of both components must be determined first.

During the first stage of the work, the two systems were thoroughly characterized, monitoring power consumption and temperature regimes to establish the correct correlation between these variables. Complementing the experimental work a thermodynamic simulation model for the absorption process was implemented to validate results and predict long-term behavior. Similarly, to predict bubble pump behavior as function of thermal oil temperature, a simple thermal simulation model was used.

Temperatures were measured using Type-K thermocouples. In the case of the fridge, the temperature sensors were distributed at different points of the cycle as shown in Fig. 1 (black dots). Due to the need of simultaneously sampling 23 different measuring points, three logging units were employed, two 4018M ADAM modules and a Schlumberger MAC 19 of German origin. Data recording was performed every 1 min during transient regimes or every 15 min

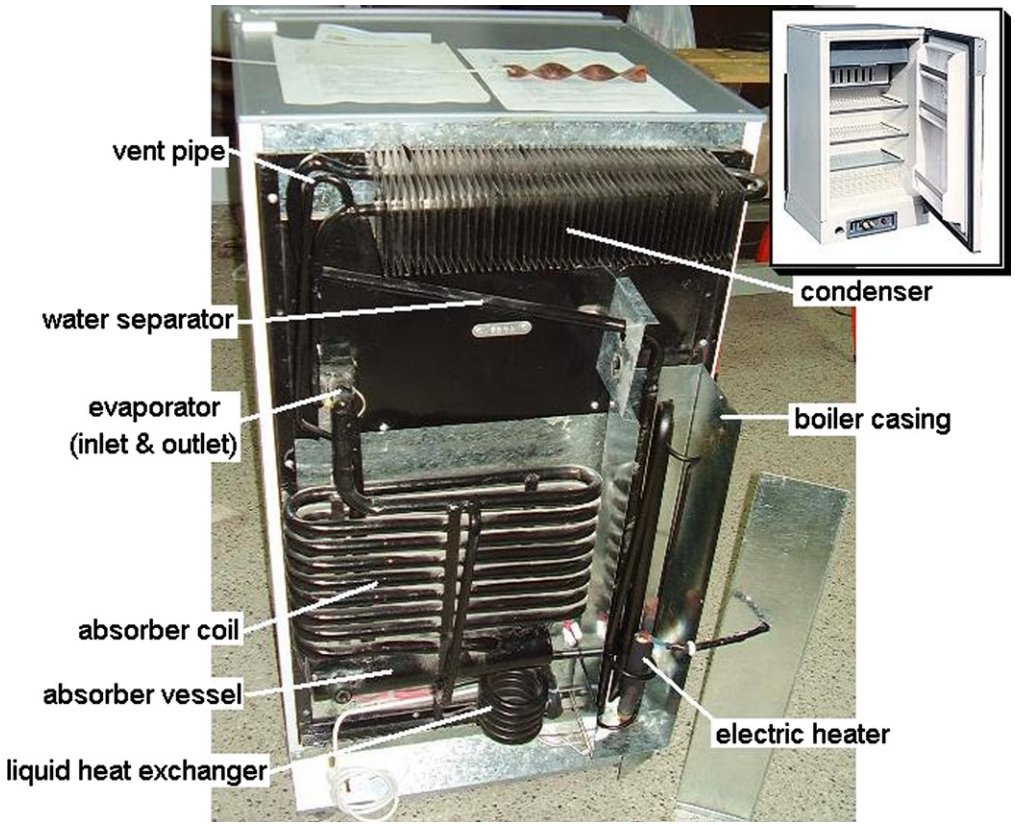

Fig. 4 – Photograph of the rear view of the refrigerator with a detail of the different cycle components. Inset: front view of the refrigerator.

otherwise. Data downloading to PC was done via the serial port using the RS232 converter appropriate to each logging device. For simplicity during characterization tests the fridge was powered with 220 V AC taken directly from the network. The power supplied to the heater was varied in a range of 240 W–100 W in order to study the dependence of the cycle with this variable. The electric power was measured by a Hioki 3131 wattmeter with analog output connected to the MAC 19.

In the case of the concentrator the temperature sensors were placed in direct contact with the thermal fluid. The recorded temperatures were: ambient temperature, input and output thermal fluid temperature at the coil, input and output thermal fluid temperature at the intermediary tank and average intermediary tank temperature. Solar radiation was measured with a photovoltaic solarimeter manufactured by GES – Grupo de Energía Solar of the CNEA (Comisión Nacional de Energía Atómica) with calibration constant 3.2 × 10-6 V W^{-1} m^{-2}. The flow rate of the fluid was controlled by means of a revolutions-per-minute (rpm) counter mounted at one end of the gear shaft driving the pump. The rpm was

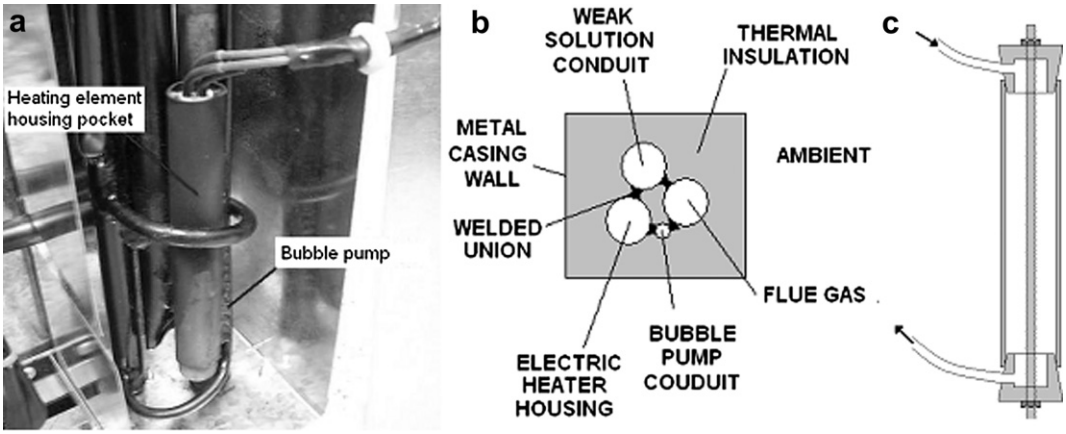

Fig. 5 – a) Partial view of the generator. b) Schematic diagram of the thermal link between components of the generator. c) heat exchanger arrangement.

varied by changing the voltage supplied to the driving DC motor. Volumetric flow rate was determined by measuring the time it takes for the pump to fill up a 1 L beaker. For each selected rpm point a series of ten volumetric flow measurements was performed and the resulting average value was taken as the most representative. In this way a calibration curve (rpm vs. volumetric flow rate) was determined prior to testing with average volumetric flow rates between 11 and 60 l h^{-1}. The gear pump used has the advantage of displacing a constant volume no matter the density of the fluid. The dependence of thermal fluid density with temperature was taken into account for correction when determining the corresponding mass flow rate.

5. Modeling

5.1. *Thermodynamic model of the cycle*

The cycle was modeled using a diagram of interconnected components to analyze the flow of energy and mass between them as detailed in Fig. 6. The model uses the measured values of the temperatures at the inlet and outlet of each component, as input data for the determination of the thermodynamic properties of the fluids in the circuit. Given that operational pressure of the cycle and the molar fractions of rich and weak solutions are unknown these properties are used as variable parameters to fit the experimental temperatures to those predicted by the model.

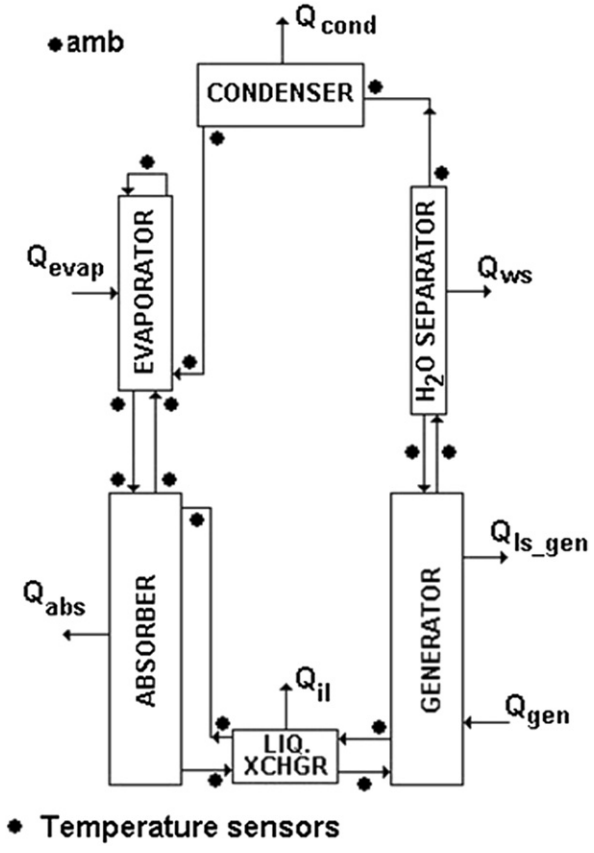

Fig. 6 – Distribution of temperature sensors.

The assumptions made in the model are: a) substances in gaseous phase behave like uncompressible ideal gas; b) the homogeneous mixture of the substances involved follows Raoult's law. c) The thermodynamic properties of the ammonia-water mixture at different points in the circuit were determined using the vapor/liquid equilibrium approximation functions developed by Patek and Klomfar (1995).

Assuming the gas phase to be an ideal mixture of real components, the specific enthalpy $h_g(T, y)$ can be calculated from the enthalpy $h_{Am}(T, p)$ and $h_W(T, p)$ of pure ammonia and water:

$$h_g(T,y) = (1-w)h_W(T,p) + w \cdot h_{Am}(T,p) \tag{1}$$

where

$$w = \frac{yM_{Am}}{yM_{Am} + (1-y)M_W} \tag{2}$$

The pressure p in eq. (1) corresponds to the operating cycle pressure which is unknown therefore it is taken as a variable parameter when fitting the experimental data.

The thermodynamic functions used for the calculations are:

$$T(p,x) = T_0 \sum_i a_i (1-x)^{m_i} \left[\ln\left(\frac{p_0}{p}\right)\right]^{n_i} \tag{3}$$

$$T(p,y) = T_0 \sum_i a_i (1-y)^{m_i/4} \left[\ln\left(\frac{p_0}{p}\right)\right]^{n_i} \tag{4}$$

$$y(p,x) = 1 - \exp\left[\ln(1-x)\sum_i a_i \left(\frac{p}{p_0}\right)^{m_i} x^{n_i/3}\right] \tag{5}$$

$$h_l(T,x) = h_0 \sum_i a_i \left(\frac{T}{T_0} - 1\right)^{m_i} x^{n_i} \tag{6}$$

$$h_g(T,y) = h_0 \sum_i a_i \left(1 - \frac{T}{T_0}\right)^{m_i} (1-y)^{n_i/4} \tag{7}$$

where p, x and y are used as variable parameters to minimize the difference between experimental temperature and predicted temperatures. The calculation algorithm was implemented in MathCad7®.

The energy rate Q_{evap} extracted by the evaporator is an important parameter that need to be known either for modeling purposes or for the determination of the coefficient of performance (COP) of the cycle. During operation, the evaporator must extract energy from inside the cabinet at a rate that under steady state conditions compensates the rate of energy gain from the environment. This rate of energy gain can be calculated knowing the surface temperature of the inner and outer sides of the cabinet wall, and the thickness and thermal conductivity of the insulation material of the cabinet wall using the expression valid for heat conduction through a wall (Welty, 1978):

$$q = -kA\frac{\Delta T}{\Delta X} \tag{8}$$

For a real cooling cycle the COP is defined as:

$$COP_{real} = \frac{Q_{evap}}{Q_{total}} \tag{9}$$

Where Q_{total} includes any losses that may exist in the heat source (generator unit).

Because the generator unit is surrounded by thermal insulation and housed in an enclosure of galvanized metal walls Eq. (8) can also be applied to estimate the heat loss Q_{ls_gen} of the heat source (generator unit). Consequently, the mean temperature of the generator unit, the surface temperature of the outer side of the enclosure wall, the thickness and thermal conductivity of the insulation are all variables that must be known.

5.2. *Thermal model for the generator unit*

The modeling of the generator unit under steady state conditions could allow predicting the expected bubble pump temperature as function of the thermal heat transfer fluid temperature when using oil as heat source. The proposed thermal model was compared with the experimental data gathered during tests using LPG burner or the electric heater as heat source. Fig. 5b shows the schematic diagram of the thermal link between components of the generator unit. The thermal model was implemented under SIMUSOL, a free distribution software developed by the INENCO - National Institute of Non-Conventional Energy of the National University of Salta, Argentina. SIMUSOL makes use of the analogy between thermal and electrical networks. The program is based on SCEPTRE and runs under Linux. The system under study must consist of concentrated elements which means it shall be defined by a finite number of temperatures. Elements must be in contact with pairs of temperatures and must transfer energy between them.

Table 2 describes parameters and magnitudes used for the elements of the circuit. The mass flow rates of the weak and strong solutions used in the calculations are those resulting from the thermodynamic model of the cycle described in 5.1. The prediction of the model as compared to experimental measurements is discussed in 6.3.

6. Experimental results

6.1. *Fridge characterization*

The results obtained during the characterization of the refrigerator are presented in this section and the corresponding testing conditions are summarized in Table 3.

6.1.1. *Empty fridge (summer)*

The first test was carried out during 8 days with the fridge completely empty. During this time interval the power supplied to the heater of the generator unit (Q_{gen}) was varied from 250 W to 105 W. Fig. 7 shows the time evolution curves for some of the variables measured. T_{av_cab} was measured in the geometric center of the inner volume of the cabinet. The events in the graph worth mentioning are: (A) a transient startup process taking approximately 6 h before steady state conditions are reached; (B) a network power cutoff; (C) the setup of a decay process in the cycle induced by lowering the power supplied to the heater below a minimum level needed to maintain optimal operation conditions; (D) the opening of the fridge door; (E-F) a power shut down or drop down below 100 W which induce the collapse of the cycle with temperatures that converge to T_{amb}; (G) ceiling fan of the laboratory turned on. Performance is improved due to more efficient heat transfer rates to ambient at the condenser and absorber.

In addition, the observable phenomena worth mentioning are:

a) T_{amb} remained steady at ~31 °C during the test.

b) for $Q_{gen} > 240$ W the water separator temperature (T_{ws}) sets around 121 °C quite insensitive to variations in the electric power injection to the heater indicating a stable equilibrium desorption rate has been reached in the generator unit. On the contrary, for $Q_{gen} < 200$ W T_{ws} shows greater dependency with power variations practically replicating the features of the Q_{gen} curve when power drops below 130 W. Defining the ratio temperature-to-power variations between the water separator and generator as:

$$\varepsilon = \frac{\Delta T_{ws}}{\Delta Q_{gen}} \tag{10}$$

This ratio increases with decreasing Q_{gen} with values of 0.11 °C W^{-1}, 0.24 °C W^{-1} and 0.77 °C W^{-1} for the power intervals >240 W, <200 W and <130 W respectively.

c) For $Q_{gen} < 100$ W the cycle is driven to collapse.

Table 2 – Description of parameters and magnitudes used in the simulation of the generator unit.

	Generator	Electric heating element	Bubble pump (weak solution)	Strong solution
Dimensions: Diameter	0.024 m	0.024 m	0.008 m	0.024 m
Height	0.15 m	0.15 m	0.15 m	0.15 m
Thermal conductivity	Fe 80 W/m°C	Fe 80 W/m°C Cu 386 W/m°C	Fe 80 W/m°C	Fe 80 W/m°C
Filling substance	Air	Copper Thermal oil	15% Ammonia solution	30% Ammonia solution
Heat Capacity	4186 J/kg°C	Cu: 390 J/kg. °C Aceite: 2540 J/kg°C	4580 J/kg°C	4700 J/kg°C
Density	Air (@210 °C): 0.616 kg/m^3	Cu: 8960 kg/m^3 Thermal Oil: 763.33 kg/m^3	950 kg/m^3	820 kg/m^3
Mass flow rate (as estimated by the thermodynamic model of the cycle)	–	–	0.00013 kg/seg	0.00016 kg/seg

Table 3 – Description of testing conditions.

Test condition	Ambient condition	Test duration	Power injection	Power source
Empty	Summer Tamb = ~31 °C	8 days	250 W–105 W	Electricity
Loaded – 32 L of water	Summer Tamb = ~32 °C	32 days	250 W–130 W	Electricity
Loaded – 32 L of water	Winter Tamb = ~18 °C	34 days	230 W–103 W	Electricity
Loaded – 32 L of water	Autumn Tamb = ~21 °C	10–15 days	620 gr/h	Gas

d) When the cycle begins to degrade (C) T_{evap} rises from −18.5 °C to −10 °C with the consequent increase of T_{av_cab} from ~1 °C to 7 °C.

e) The fluctuations in Q_{gen} were caused by natural daily variations on the supply voltage of the network of the building where the laboratory is located.

6.1.2. *Loaded fridge (summer)*

The test was carried out with the fridge loaded with 32 L of water contained in PET bottles. Similar findings to those obtained with fridge empty are observed. However, two new comments can be made:

a) A decrease of T_{amb} from 32 °C to 27 °C caused T_{evap} and T_{av_cab} to fall down reaching −20 °C and 0 °C respectively (A). This effect is a consequence of lower heat flux from the ambient inwards. This energy gain can be further reduced by improving the thermal insulation of the cabinet wall.
b) A decrease of ~45% in Q_{gen} (to ~137 W) caused T_{av_cab} to increase to 7 °C temperature which in the case of the test with empty fridge was reached for a power injection of about 105 W. This same final state for different power injection level is due to the lack of thermal load inside the cabinet hence less energy is required to maintain inner thermal conditions. Moreover, ε presents the same dependency with Q_{gen} as previously found.

6.1.3. *Loaded fridge (winter)*

Fig. 8 shows the results of a test conducted during winter with average T_{amb} of ~18 °C. Due to lower heat input from the environment T_{evap}, T_{fr} and T_{av_cab} of −23 °C, −10 °C and −5 °C respectively were maintained throughout almost the entire test. It can also be observed in Fig. 8 that although T_{ws} dropped by more than ~20 °C with respect to previous tests (Fig. 7) the cycle remained stable even with a reduction of ~40% in Q_{gen} (to ~140 W). Under these circumstances the degradation of the cycle starts to show up for Q_{gen} ~103 W. This finding lead to the development of an electric energy economizer for the heater of the fridge which was implemented and successfully tested (Cáceres et al., 2009). As found before, ε exhibits the same dependency with Q_{gen}.

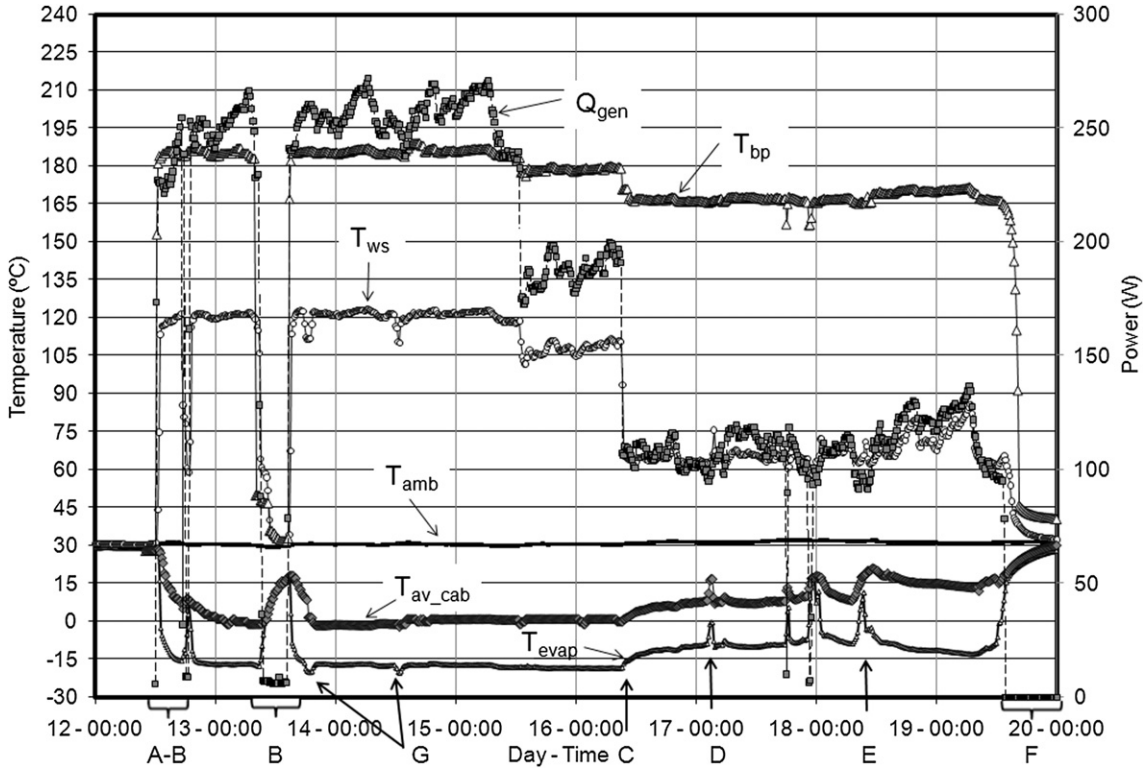

Fig. 7 – Time evolution curves for a summer test with the fridge empty.

Fig. 9 is the resulting graph of ε as a function of Q_{gen} for all tests performed. Superimposed is the resulting regression line which, eventually, can be used in a control algorithm to estimate T_{ws} for a given Q_{gen} and predict the stability of the cycle.

A common feature of all tests carried out is that T_{bp} remained above 175 °C except for energy injection rates at which the cycle begins to collapse hence falling below 165 °C.

6.1.4. *Loaded fridge – gas consumption*

To determine gas consumption the fridge was powered using the LPG burner. Propane gas was supplied by 10 kg domestic gas cylinder which was subject to periodic weighting; at the beginning of the test and daily; to trace weight loss. An average gas consumption of 620 g per day (358 W) was obtained from tests performed with different duration (10 and 15 days) representing 1.6 times more than the consumption reported by the manufacturer.

For the determination of the COP the energy extraction rate at the evaporator was estimated from experimental data corresponding to the transient period of the cycle between startup and steady state. During this phase the evaporator must extract energy from inside the cabinet at a rate that under steady state conditions compensates the rate of energy gain from the environment, this is, once steady state is reached $Q_{evap} = Q_{gain}$. Moreover, Q_{gain} calculated using Eq. (8) for both cases empty and loaded fridge led to 36.7 W. Furthermore, Q_{total} is equal to Q_{gen}, energy injection rate experimentally measured and recorded with the wattmeter. Therefore, replacing Q_{evap} and Q_{gen} in Eq. (9) results in a COP of ~0.18, in good agreement with what is reported in literature for this type of small absorption units (Isaza, 2004).

In order to determine the COP using the thermodynamic model proposed previously system parameters (system pressure, weak and strong ammonia solution concentrations) must all be known beforehand. For this purpose, a parametric fitting was carried out between predicted temperatures and the experimental temperatures using with system pressure, weak and rich solution concentrations as variable parameters. As result a cycle working pressure of 25 bar and weak and strong ammonia solution concentrations of 30% and 15% respectively were obtained. These values are consistent with those reported in the literature by different authors for this type of cycle (Kwan et al., 1995; Isaza, 2004; Patek and Klomfar, 1995; Almén). Fig. 10 shows the comparison between experimental and predicted COP. The analysis was performed for data points at which the cycle was under steady state conditions. The differences observed may be due to experimental errors as temperatures are measured on the outside of the ducts. The largest deviations present in the plot may correspond to experimental states of the ammonia-water mixture that fall outside the range of validity of the thermodynamic properties curves used in the model (Patek and Klomfar, 1995). Similarly, Fig. 10 also shows the good agreement obtained when comparing measured power injection, Q_{gen}, with the power injection estimated with the model corrected to account for heat losses in the generator. This heat loss, Q_{ls_gen}, was estimated using Eq. (8) and the measured temperatures of the generator unit leading to 34.2 W. The average error in these comparisons is within 8.5%.

6.2. *PC characterization*

PC Tests were performed during different months of the year, February to August, and under different weather conditions, clear skies to partly cloudy. Focusing was done manually according to demand in order to keep T_{out} as high as possible. Flow rate of the thermal fluid in the hydraulic circuit was varied from 8 l h^{-1} to 15 l h^{-1} Fig. 11 shows typical response

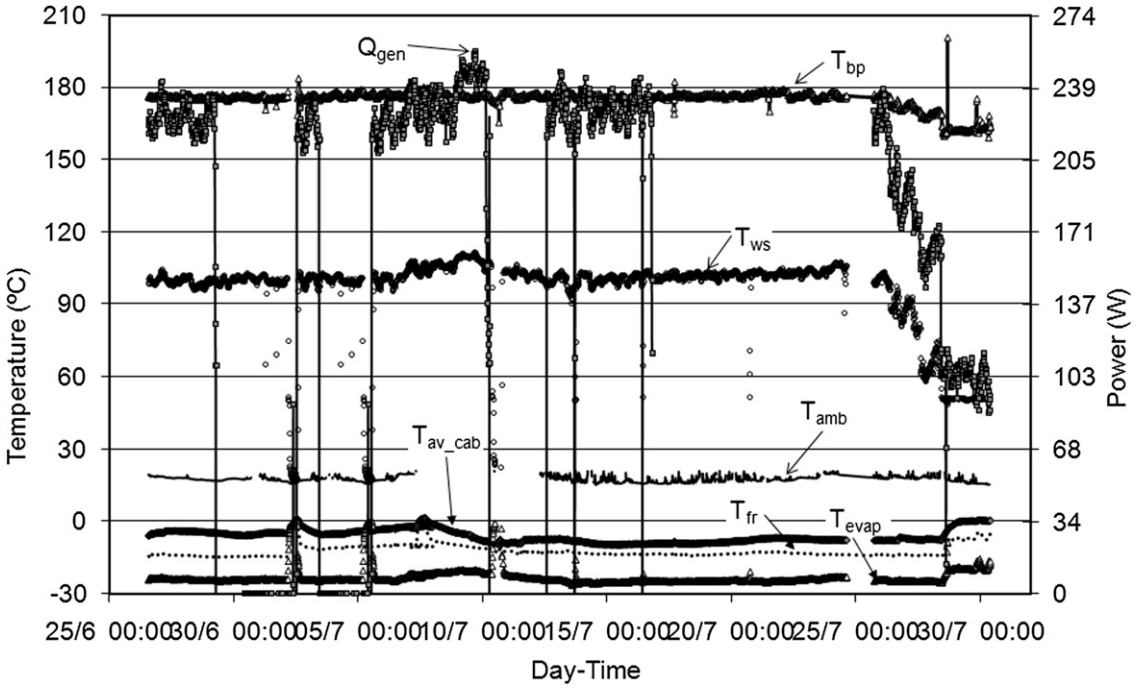

Fig. 8 – Time evolution curves for a summer test with the fridge loaded with 32 l of water.

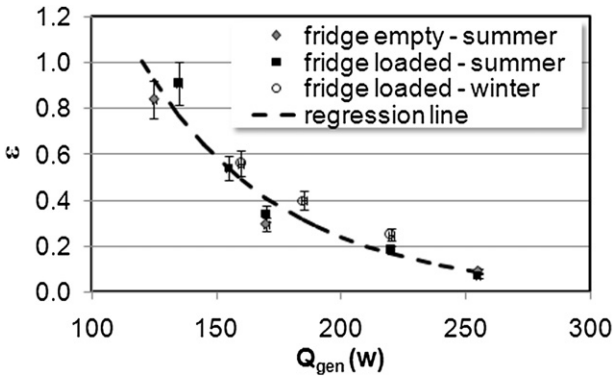

Fig. 9 – Dependency of the ratio temperature-to-power variations (ϵ) for water separator and generator unit on Q_{gen}.

curves obtained for a test conducted in a sunny winter day with a flow rate of ~12 l h^{-1}. The sudden drops in T_{out} were caused by the lack of continuous sun tracking. This is explained by the fact that the concentrator used was originally designed for cooking purposes with a cube shaped oven (0.4 × 0.4 × 0.4 m) acting as receiver in its focus. This configuration requires to be refocused approximately every 40 min without causing appreciable change in the temperatures inside the oven. In contrast, the smaller dimensions of the cylindrical shape receiver used (see Fig. 2) make it very focus-sensitive so as to need refocusing at intervals of 5 min maximum to maintain a stable temperature regime. Even with this defocusing problem T_{out} remained above 175 °C for almost 4 h, a general a result common to all PC tests performed thus indicating that the system is able to provide enough power and, in principle, enough temperature to energize the refrigeration cycle. This holds true under the assumption that a T_{bp} of at least 165 °C is required for the cycle to operate as it came out from the previous fridge characterization results described in 6.1. Moreover, a PC average efficiency of ~26% was obtained from these tests.

Fig. 12 presents the resulting curves for a test carried out on a clear sky summer day with a flow rate of ~8 l h^{-1}. Care was taken to maintain the system focused so as to get an output temperature as steady as possible. In this manner T_{out} was kept above 200 °C for almost 6 h. As result an average useful power and efficiency of 530 W and 28% respectively were determined for the PC.

6.3. *Hot oil as heat source*

In these experiments the heat exchanger of the fridge is connected directly to the intermediary tank and the entire hydraulic circuit is filled with heat transfer oil. The thermal fluid is heated to 250 °C and forced to circulate in the system aided by the electric heater and gear pump located inside the intermediary tank. In the first test main components reached temperatures comparable to those corresponding to stable cycle operation as measured during fridge characterization tests (T_{bp} ~ 165 °C; T_{ws} ~ 120 °C; T_{av_hx} ~ 225 °C; T_{fg} ~ 300 °C). Nevertheless, the cycle failed to start with T_{ev} falling occasionally to minimums of 0 °C. As already mentioned the refrigerator operates solely by the heat applied to the generator unit and it is of paramount importance for its operation that this heat be maintained within the necessary limits as well as be properly distributed to assure correct operational temperatures throughout the different components of the generator unit. The results obtained are a clear indication that

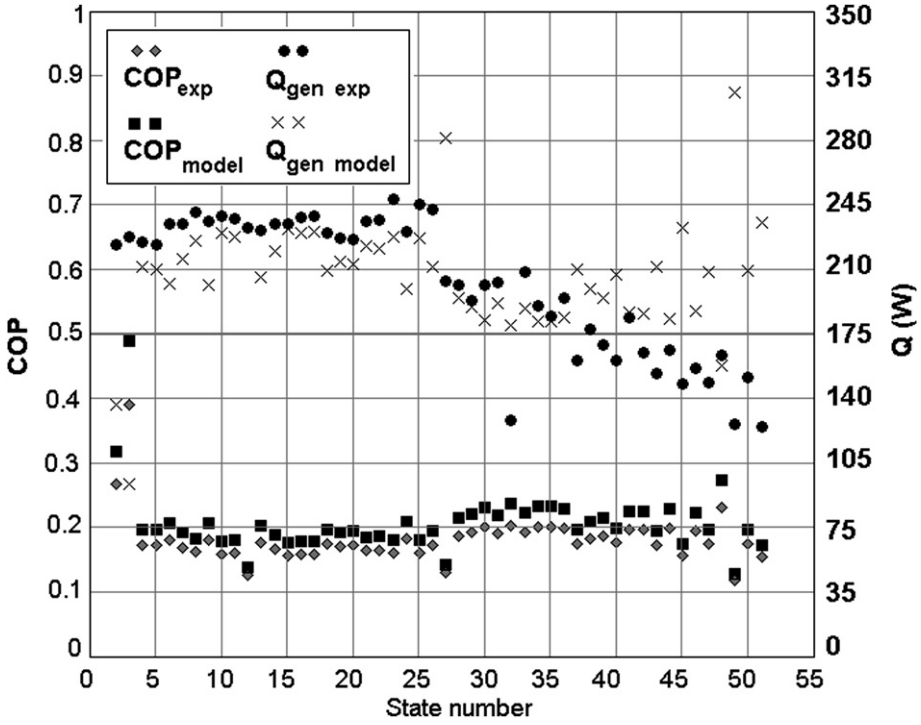

Fig. 10 – Comparison between experimental and predicted COP and power injection.

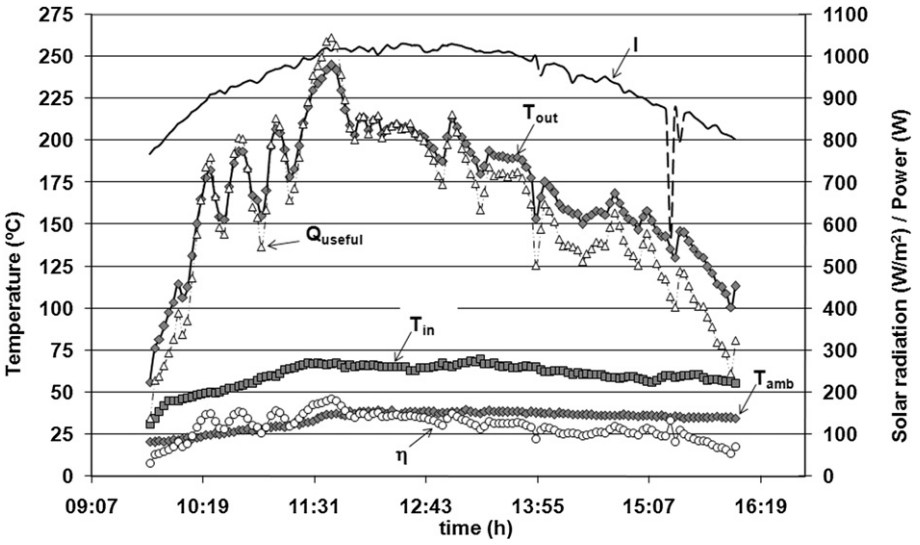

Fig. 11 – PC time evolution of variables during a test in winter.

the heat source used does not fulfill these requirements. It is a fact that thermal energy from either source (electric heater or GLP burner) is transferred to the bubble pump and consequently to the generator through a narrow welded region with a length of approximately 0.15 m (Fig. 5b) thus making the heat transfer processes rather ineffective with high heat losses. The heat losses are counterbalanced by raising the temperature of the heat source to 350 °C as it is the case with the heat sources provided with the equipment under test.

An estimation of T_{bp} as a function of T_{av_hx} under steady state conditions was done using the thermal simulation model of the generator unit described in 4.1. When Tav_hx = 220 °C the model predicts a Tbp = 170 °C, in good agreement with the experimental outcome as it can be observed comparing the plot presented in the inset in Fig. 13 with the temperature values registered during testing (circles on B line).

Because T_{av_hx} is in the range of 250 °C, a temperature not high enough to activate the cycle, it was decided to start the refrigerator with the LPG burner and once operational stability is reached to switch to hot thermal oil as heat source. To speed up the startup process and minimize the heat extraction that may be caused by cold oil circulating through the heat exchanger in the generator unit the oil was simultaneously heated by the electric heater inside the intermediary tank. The objective behind this strategy was to analyze whether the cycle could be maintained operational after ensuring its stability by proper initial heat distribution with some other heat source. Fig. 13 shows the resulting time evolution curves of the variables measured during a typical test.

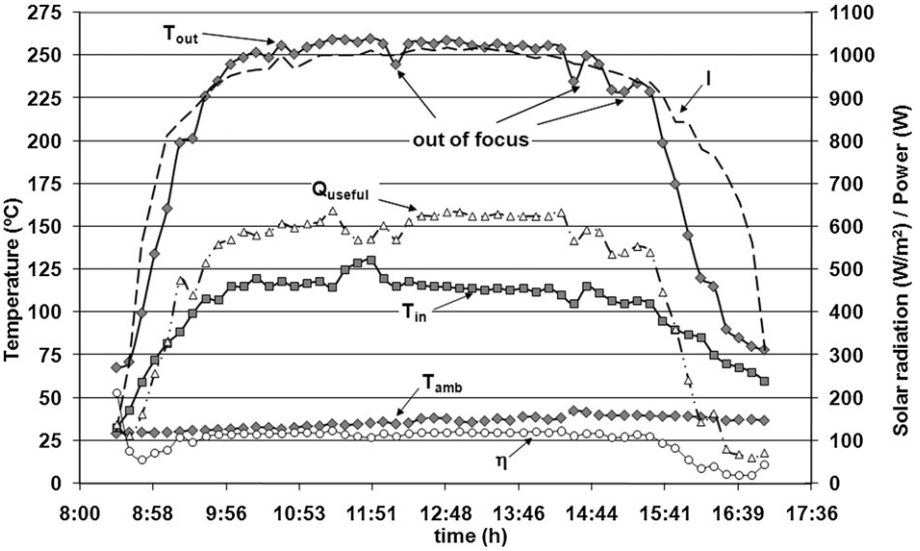

Fig. 12 – PC time evolution of variables during a test in summer with controlled sun tracking.

Four singular events are observed in the graph: A) start of cycle (LPG burner on and $P = 500$ W); B) burner off and $P = 500$ W; C) reduction of electric heater power ($P = 300$ W) and D) increase of electric heater power ($P = 750$ W).

Noticeable features during these events are:

a) T_{ws} remained below 60 °C until "A" after which the various components of the system acquire the right conditions so the cycle starts.
b) Between "A" and "B" T_{ws} remains around 120 °C while the average temperature in the evaporator drops sharply to −25 °C and stabilizes at this level.
c) At "B" the LPG burner is turned off and operation continues with hot thermal oil as the only heat source. Electric power supplied to the heater in the intermediary tank is 500 W. T_{ws} remained slightly above 60 °C and equal or slightly higher than T_{bp} without compromising the stability of the cycle.
d) At "C" the power supplied to the electric heater is reduced to 300 W T_{ws} slowly decreasing crossing down the region of 60 °C. The inertia of the system is such that the effect on cycle operation is observed after about 20 min by the increase of T_{ev}.
e) At "D" power supplied to the electric heater is increased to 750 W. Although after 30 min the system seems to recover operating conditions the state of the cycle is very unstable. Any drop of T_{ws} below T_{bp} as it happened after "C" may drive it to collapse. Furthermore, it appears that the critical temperature interval for both T_{ws} and T_{bp} where this situation is highly probable to occur is in the range of 55 °C–65 °C.

6.4. PC-Fridge coupled experiments

The PC and refrigerator were interconnected following the integration scheme proposed in Fig. 1. Due to the distance between PC relative to the location of the fridge each branch of the connecting pipes were 7 m in length (supply and return). They were thermally insulated with fiber glass wool with a thickness of 0.05 m and wrapped up in aluminum foil.

The application of the combined heat source (LPG burner/electric heater) strategy during start as previously described proved unsuccessful. Although thermally insulated, the heat losses in the connecting pipes between the PC and the heat exchanger of the fridge make impossible to keep the cycle running after the LPG burner was shut off driving the cycle to collapse in a short time.

Despite the availability of sufficient power this lower temperature heat source can not properly distribute the heat in the generator in a way to activate the cycle. However, under certain circumstances it does keep the cycle operative under very unstable conditions as it was shown in 6.3. Under these circumstances, the re-engineering of the heat exchanger in the refrigerator is a must in order to achieve the appropriate temperature distribution in the generating unit when using this low temperature heat source.

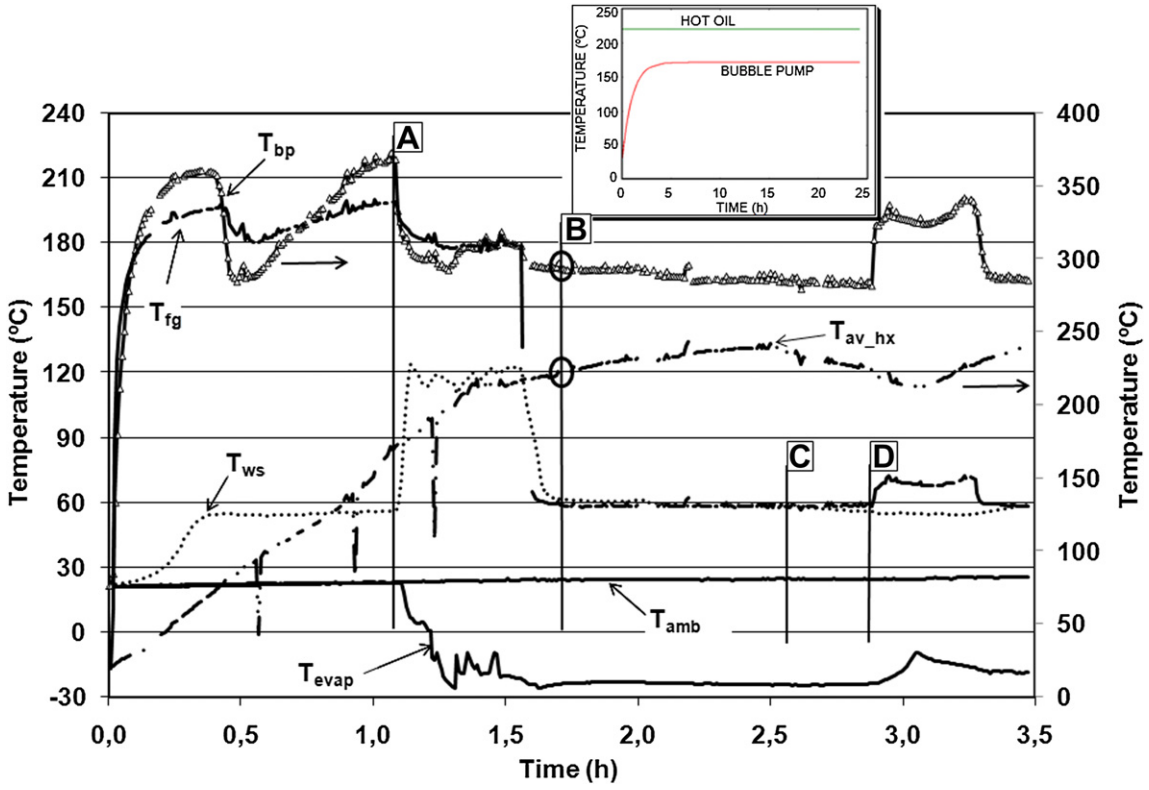

Fig. 13 – Fridge test with dual heat source gas-hot oil. Inset: outcome of the simulation model for the generator unit with hot oil at 220 °C.

7. Conclusions

The integration of a small commercial ammonia-water absorption refrigerator with a solar concentrator as heat source was theoretically and experimentally analyzed. Main conclusions drawn from the study are:

a) With a heat source of ~350 °C the temperature of the bubble pump is ~180 °C, while the temperature at the entrance of the water separator is ~120 °C. These temperatures depend on the thermal power injection and room temperature where the cycle operates.
b) Gas consumption is 1.6 times higher than that reported by the manufacturer.
c) Based on the 250 W electric heater supplied with the fridge (350 °C heat source) it was determined that the cycle remains operational even under a reduction of ~40% in the electric power injection leading to a required minimum power injection of ~120 W. Similarly, it was determined that minimum operational temperatures of about 165 °C in the bubble pump and 65 °C in the water separator must be ensured for the cycle to operate.
d) Cycle operation is very sensitive to T_{amb}. Inappropriate heat exchange rates in the absorber and condenser affect performance deteriorating T_{av_cab}.
e) Working pressure of 25 bar and weak and strong solution concentrations of 15% and 30% respectively were determined by parametric fitting experimental data using a thermodynamic model of the cycle.
f) Experimental and theoretical COP of ~0.18 was determined with an agreement within 8.5%.
g) A simple thermal model used for the generator unit proved to be useful for predicting bubble pump temperatures as function of thermal fluid temperature when hot oil is used as heat source.
h) A threshold operating temperature for T_{bp} and T_{ws} of 60 °C was determined by indoor experiments with hot oil as heat source. Despite the inappropriate heat distribution due to lower temp heat source (220 °C) it was possible to maintain the cycle running in a very unstable regime. At these threshold temperatures, T_{ws} must remain slightly above 60 °C and equal or slightly higher than T_{bp} without compromising the operation of the cycle.
i) A solar PC efficiency of about 26% was determined under testing conditions.
j) In order to keep a stable temperature regime a solar PC refocus time lower than 5 min is required.
k) It was experimentally verified that the solar PC can deliver temperatures above 200 °C for almost 6 h with an average useful power and efficiency of 530 W and 26% respectively. The inappropriate heat distribution in the generator unit due to lower temp heat source (220 °C) and the higher heat losses of the solar PC-fridge connecting pipes made unviable the cycle operation during outdoor testing.

The overall conclusion is that the integration is feasible with some re-engineering of the generator. A more effective heat transfer process between the thermal energy source and the generator unit is needed in order to be able work with lower temperatures heat sources. This aspect is currently being analyzed by one manufacturer.

Another aspect to consider is the concentrating device. As tracking is a must, a Linear Parabolic Concentrator (LPC) presents the advantage of having a stationary hydraulic circuit and tracking on one axis only, thus becoming a better choice to consider. This device can deliver similar temperature and power output as the Parabolic Concentrator as reported by Dri et al. (2009).

Because the cycle needs to operate around the clock, a proper integration scheme and control strategy should consider powering the fridge overnight with the LPG burner, and switching to solar source during the day.

Acknowledgments

Authors wish to acknowledge the Agencia Nacional de Promoción Científica y Tecnológica for funding the project PICTO 18617 which made this work possible.

Appendix. Supplementary material

Supplementary data associated with this article can be found in the online version, at doi:10.1016/j.ijrefrig.2011.07.004.

REFERENCES

Almén – Carl, G., Gas Absorption Refrigeration Technology, <http://www.absreftec.com/index.html>.
Essotherm, <http//www.essomobilborur.com/pdf/esso/industriales/essotherm500.pdf>.
Cáceres, M., Busso, A., Franco, J., 2009. Controlador de Inyección de Energía para Ciclo Frigorífico de Absorción de Amoniaco-Agua. Avances en Energías Renovables y Medio Ambiente 13.
Cadena, C., Saravia, L., 2001. Análisis del comportamiento térmico de absorbedores de aluminio empleados en cocinas solares con concentración. Avances en Energías Renovables y Medio Ambiente 5, 8.85.
Cadena, C., Saravia, L., Echazú, R., 2002. Transferencia de Calor y Curvas de Calentamiento para Absorbedores de Aluminio empleados en Cocinas Solares. Avances en Energías Renovables y Medio Ambiente 6 (1), 03.07.
Cauquen, <http://www.benco.com.uy/php/descargas/lubricantes/industriales/transferencia-termica/FDS%2520Cauquen%25201_95790_tcm15-36553.pdf>.
Chen, J., Kim, K.J., Herold, K.E., 1996. Performance enhancement of a diffusion–absorption refrigerator. Int. J. Refrigeration 19 (3), 208–218.
Dri, Fabio, Busso, Arturo, Gea, Marcelo, 2009. Ensayos de un Concentrador Solar Cilindro Parabólico con Fluido Caloportador. Avances en Energías Renovables y Medio Ambiente 13.
Echazú, R., Cadena, C., Saravia, L., 2000. Estudio de materiales reflectivos para concentradores solares. Avances en Energías Renovables y Medio Ambiente 4, 8.11–8.19.
Fan, Y., Luo, L., Souyri, B., 2007. Review of solar sorption refrigeration technologies: development and applications. Renew. Sust. Energ. Rev. 11, 1758–1775.

Gaia, R., Bessone, H., Cortés, A., 1999. Energía Solar para Refrigeración Doméstica. Avances en Energías Renovables y Medio Ambiente 3 (1), 03.17–03.20.

Herold, K.E., Rademacher, R., Klein, S.A., 1996. Absorption Chillers and Heat Pumps, first ed. CRC Press, Boca Raton, USA, ISBN 0-8493-9427-9. 235–242.

Hoyos, D., Cadena, C., Saravia, L., 1999. Determinación de la distribución de radiación incidente en el plano focal de un concentrador por procesamiento digital de imágenes. Avances en Energías Renovables y Medio Ambiente 3, 8.57.

Isaza, C.A.R., 2004. Integración De Un Refrigerador Por Absorción Doméstico A Un Sistema De Energía Solar. Jornadas Iberoamericanas sobre el Enfriamiento Solar: Tecnologías para el Desarrollo Económico y Social de la Región Iberoamericana. <http://www.riraas.net/documentacion/CD_09/CONFERENCIAS/Conferencia%2520Isaza%25203.pdf>.

Jakob, U., Eicker, U., Schneider, D., Taki, A.H., Cook, M.J., 2008. Simulation and experimental investigation into diffusion absorption cooling machines for air-conditioning applications. Appl. Therm. Eng. 28, 1138–1150.

Keith, D.F., 1927. IcyBall Patent 1,740,737. <http://crosleyautoclub.com/IcyBall/IB1740737/IB1740737.html>.

Kim, K.J., Shi, Z., Chen, J., Herold, K.E., 1995. Hotel room air conditioner design based on the diffusion–absorption cycle, ASHRAE Tech. Data Bull. 11 (2), 47–58.

Kouremenos, D.A., Stegou-Sagia, A., Antonopoulos, K.A., 1994. Three dimensional evaporation process in aqua-ammonia absorption refrigerators using helium as inert gas. Int. J. Refrigeration 17 (1), 58–67.

Kwan, J.K., Zoujun, S., Jie, C., Keith, E.H., 1995. Hotel room air conditioner design based on the diffusion-absorption cycle. Dessicant and absorption cooling. ASHRAE Tech. Data Bull. 11 (2), 47–58.

Patek, J., Klomfar, J., 1995. Simple functions for fast calculation of selected thermodynamic properties of ammonia-water system. Int. J. Refrigeration 18 (4), 228–234.

Saravia, L., Suárez, H., 2000. Testeo de materiales reflectores para cocinas solares de tipo caja. Avances en Energías Renovables y Medio Ambiente 4, 8.75.

Saravia, L., 2002. Concentrador con doble reflexión para cocina solar. Avances en Energías Renovables y Medio Ambiente 6 (1), 3.01.

Saravia, L., Cadena, C., Caso, R., Fernández, R., 2004a. Concentrador de Distancia focal Corta para cocinas Comunales. Avances en Energías Renovables y Medio Ambiente 8 (1).

Saravia, L., Franco, J., Cadena, C., Caso, R., Fernández, C., 2004b. Múltiple use comunal solar cooker. Solar Energy 77 (2), 217–223.

Sceptre, <http://alpha.fh-friedberg.de/iem/84.html>.

Simusol, <http://www.simusol.org.ar/index.html>.

Smirnov, G.F., Bukraba, M.A., Fattuh, T., Nabulsi, B., 1996. Domestic refrigerators with absorption–diffusion units and heat-transfer panels. Int. J. Refrigeration 19 (8), 517–521.

Srikhirin, P., Aphornratana, S., 2002. Investigation of a diffusion absorption refrigerator. Appl. Therm. Eng. 22 (11), 1181–1193.

Vicatos, G., 2000. Experimental investigation on a three-fluid absorption refrigeration machine. Proc. Inst. Mech. Eng. (Part E) 214 (3), 157–172.

Welty, J., 1978. Transferencia de Calor Aplicada a la Ingeniería. Editorial Limusa.